FEBS Letters 588 (2014) 936–941

FEBS Letters
journal homepage: www.FEBSLetters.org

Competing aggregation pathways for monoclonal antibodies

Haixia Wu [a,b], Rachel Kroe-Barrett [b], Sanjaya Singh [b], Anne S. Robinson [c,d], Christopher J. Roberts [d,*]

[a] Department of Chemistry and Biochemistry, University of Delaware, Newark, DE 19711, USA
[b] Department of Biotherapeutics, Boehringer Ingelheim Pharmaceuticals, Inc., Ridgefield, CT 06877, USA
[c] Department of Chemical and Biomolecular Engineering, Tulane University, New Orleans, LA 70118, USA
[d] Department of Chemical and Biomolecular Engineering, University of Delaware, Newark, DE 19711, USA

ARTICLE INFO

Article history:
Received 14 October 2013
Revised 30 December 2013
Accepted 24 January 2014
Available online 12 February 2014

Edited by Jesus Avila

Keywords:
MAb
Aggregation
Hot-spot

ABSTRACT

Aggregation is mediated by local unfolding to allow aggregation "hot spot(s)" to become solvent exposed and available to associate with a hot spot on another partially unfolded protein. Historically, the unfolding of either the crystallizable fragment (Fc) or the antigen binding fragment (Fab) regions of a given monoclonal antibody (MAb) has been implicated in aggregation, with differing results across different proteins. The present work focuses on separately quantifying the aggregation kinetics of isolated Fc, isolated Fab, and intact MAb as a function of pH under accelerated (high temperature) conditions. The results show that both Fab and Fc are aggregation prone and compete within the same MAb.

1. Introduction

Monoclonal antibody (MAb or immunoglobulin gamma, IgG) and MAb-based proteins, such as antigen-binding fragments (Fab), single-chain variable fragments, and multi-specific scaffolds such as antibody-drug conjugates, represent one of the largest growing class of proteins in the pharmaceutical and biotechnology industries [1]. One of the major concerns associated with successful delivery of protein therapeutics to patients is non-native aggregates that can form during in vivo expression, purification and processing, as well as upon storage and administration. Aggregates in formulated therapeutic products can cause unwanted immune responses and loss of biological activity [2,3]. While most therapeutic MAbs are formulated at pH values between 5 and 7 [4], key processing steps such as viral inactivation and elution from certain affinity-chromatography resins occur at much more acidic conditions [5,6].

Non-native aggregation (hereafter simply denoted as aggregation) denotes any process of forming aggregates that are composed of proteins that have lost some or all of their native or folded structure; this often will also be accompanied by an increase in inter-protein beta-sheet structures that help to stabilize the aggregates [7]. The resulting aggregates are typically irreversible under the solvent conditions that they form. As a result, one must control the net aggregation rate in order to minimize aggregate formation [8].

Monomers within the aggregates are conjectured to "bind" to one another via "hot spot" sequences that contain relatively large amounts of hydrophobic amino acids that have a high propensity to form beta-sheet structures that provide stabilizing inter-protein hydrogen bonds, by analogy with polypeptide aggregation [9–11]. The exact location or sequence identity of such hydrophobic "patches" or hot spots has been experimentally determined for many polypeptides [12–15], but only for a few folded proteins [16–18], and for monoclonal antibodies has only been speculated upon based on analogies with smaller polypeptide systems [19–21]. Hydrophobic patches have been identified on the surface of some MAbs, and in some cases mutations to those regions have resulted in reduced aggregation rates [22,23].

As the "hot spot" sequences are expected to be highly hydrophobic, they are typically buried within the folded structure of soluble proteins, and thus the partially or fully unfolded monomer state is the "reactive" one with respect to aggregation. It is difficult to experimentally determine exactly what stretches of amino acids constitute the "hot spot" for most folded proteins, because they are anticipated to be relatively small stretches of sequence [21,19] and performing exhaustive mutagenesis experiments across the full

Abbreviations: Fab, antigen binding fragment; Fc, crystallizable fragment; MAb, monoclonal antibody

* Corresponding author.
E-mail address: cjr@udel.edu (C.J. Roberts).

http://dx.doi.org/10.1016/j.febslet.2014.01.051
0014-5793/

protein sequence is often impractical with large proteins such as antibodies.

The most common strategies to minimize aggregation rates are either to control key solvent conditions such as pH and temperature [24,25], or to try to identify the "hot spots" and remove them by altering those sequences [21,19]. The former is based, at least in part, on the idea that changing the solvent conditions changes the conformational stability or unfolding free energy of the monomeric protein, and this alters the effective concentration or fractional population of the unfolded or partially unfolded species that are most reactive with respect to aggregation. The latter strategy is motivated by the idea of eliminating or reducing the intrinsic aggregation propensity of the unfolded or partially unfolded monomer state [26]. The net or observed rate coefficient for aggregation (k_{obs}) is therefore proportional to the fraction or population of unfolded monomers and the intrinsic rate coefficient (k_{int}) that one would obtain if all monomers were sufficiently unfolded to reveal their aggregation-prone "hot spot(s)" [8].

A human IgG consists of two identical light chains (MW ~ 25 kDa) and two identical heavy chains (MW ~ 50 kDa) held together by disulfide bridges. Four polypeptide chains oligomerize to form a heterotetramer antibody (MW ~ 150 kDa). Each IgG heavy chain contains a variable domain (V_H), and three conserved domains: C_H1, C_H2, and C_H3 [27]. An IgG light chain is composed of a single variable domain (V_L) and a single constant domain (C_L). The V_H and C_H1 domains form heterodimers with the light chain V_L and C_L domains to create the Fab (Fragment, antigen binding) domain. The C_H2 and C_H3 domains can also be isolated together as the Fc (Fragment, crystallizable) fragment, with the Fab domains being removed via proteolysis [28,29]. The term monoclonal antibody (MAb) is synonymous with the gamma family of immunoglobulins or IgGs, and denotes any of the four IgG subclasses (IgG1–IgG4).

Previous work with human MAbs has suggested that MAb aggregation may be mediated primarily by unfolding of the C_H2 domain [30–32] or Fab domain [25,33], depending on which monoclonal antibody was being considered. Computational tools based on aggregation of small polypeptides have been used to predict that multiple "hot spots" may be possible in a human MAb [21,19]. However there is no experimental data to show that several aggregation hot-spots co-exist in a given monoclonal antibody, or that any or all become sufficiently exposed upon unfolding so as to drive aggregation on practical time scales. The present report focuses on the relative conformational stability and aggregation kinetics of a humanized MAb and its corresponding Fab and Fc fragments at acidic to near-neutral pH conditions and accelerated (elevated) temperatures. The particular humanized MAb was derived from a mouse monoclonal antibody raised against the extracellular domain of human CD40, which is a 48kDa type I membrane glycoprotein of the TNF receptor superfamily and is expressed on immune cells such as B cells, monocytes, macrophages and dendritic cells as well as on various other cell types including endothelial cells, epithelial cells (e.g., keratinocytes), fibroblasts (e.g., synoviocytes) and platelets [34]. The resulting antibody is referred to simply as MAb in the remainder of this report.

Conditions were selected such that k_{int} is measureable for some of the domains/fragments, and could be semi-quantitatively inferred for the others. This permits a direct experimental comparison of the aggregation rates for intact MAb vs. its fragments, as well as elucidation of the basis for a switch in aggregation-prone state with changing pH. To the best of our knowledge this is the first time that all aggregation rates have been shown for the same MAb, rather than comparing different MAbs or comparing disparate solution conditions. The results also illustrate the importance of considering multiple competing species and pathways when attempting to mitigate protein aggregation via either controlling the solution conditions or utilizing protein engineering to remove "hot spots".

2. Materials and methods

The IgG1 was produced at Boehringer Ingelheim Pharmaceuticals, Inc. Details regarding production of this MAb, Fab and Fc fragments, sample preparation and analysis for aggregation and unfolding experiments, and biophysical characterization of monomeric protein samples are provided in the Supplementary material. In what follows, MAb is used to denote the particular IgG1 that is the focus of this report.

3. Results and discussion

Fig. 1 shows illustrative SDS–PAGE results for digested and purified MAb fragments. There are clear bands around 47kDa and 58kDa in the non-reduced (NR) SDS–PAGE that represent the Fab and Fc fragments, respectively, purified from size exclusion chromatography (SEC). Two bands around 27kDa and 20kDa are observed in reduced (R) SDS–PAGE of the Fab fragment, and represent heavy chain (HC) and light chain (LC) components of the Fab fragment. One clear band around 29kDa observed in the reduced SDS–PAGE of Fc fragment corresponds to the HC from the Fc fragment. The observed bands in reduced and non-reduced SDS–PAGE confirm the identity and purity of Fab and Fc fragments prepared from the cleavage of the MAb by Endoproteinase Lys-C followed by SEC.

The Fab and Fc fragments, as well as the intact MAb, were each tested in differential scanning calorimetry (DSC) to compare their conformational stability and unfolding transition(s). Fig. 2 shows representative thermograms for each species as a function of temperature (T). The main panel shows the thermal unfolding curves for intact MAb, and its corresponding Fab and Fc fragments at pH 4 (panel A) and pH 6 (panel B). The intact MAb shows two broad endotherms (peaks) at pH 4, and a shoulder next to the large peak at pH 6. The Fab shows a single peak at each pH, while the Fc shows two peaks. The molar concentration of the Fab was double that of the Fc, so as to make alignment with the thermogram from the MAb more straightforward.

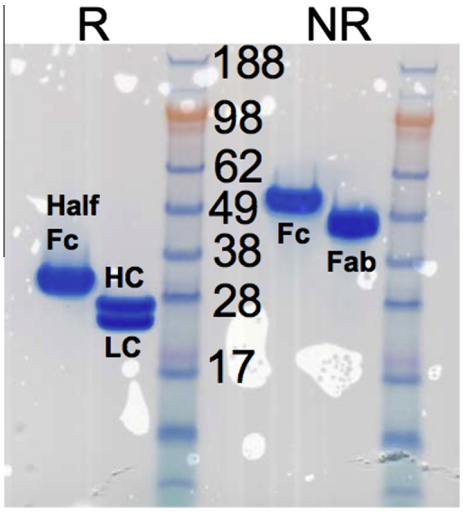

Fig. 1. Reduced (R) and non-reduced (NR) SDS–PAGE of the Fab and Fc fragments prepared from the cleavage of the MAb by Endoproteinase Lys-C followed by size exclusion purification via FPLC.

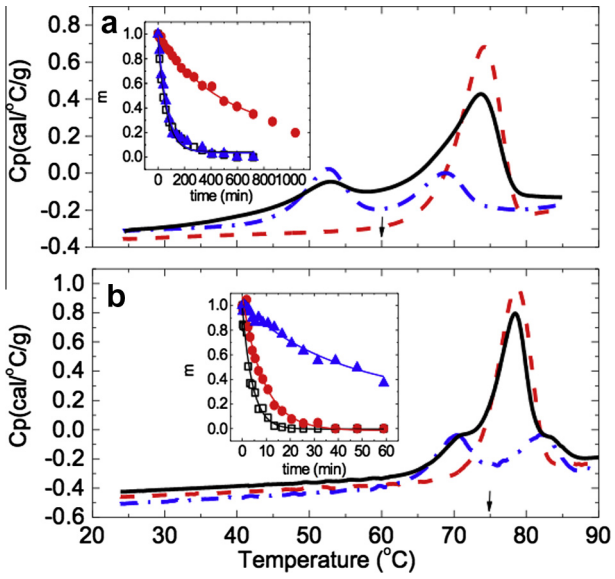

Fig. 2. Main panel: DSC curves of the intact MAb (black solid line), Fab fragment (red dashed line) and Fc fragment (blue dash-dotted line) at (a) pH 4 and (b) pH 6. Insets: monomer loss as a function of incubation time for the intact MAb (black open squares), Fab fragment (red solid circles) and Fc fragment (blue solid triangles) at the same pH as the main panel. The solid lines are first-order exponential fits to interpolate the half-life t_{50}. Incubation temperatures for the insets are (a) 60 °C and (b) 75 °C as marked by the vertical black arrows in the main panels. The molar concentrations for main panels and insets is 13.3 μM for the MAb and Fc-fragment results, and 26.6 μM for the Fab.

It has been shown previously for the IgG1 subclass that the lower-T endotherm for the Fc fragment under similar solution conditions corresponds to unfolding of the C_H2 domain, while the higher-T peak results from unfolding of C_H3 domain [28,35,36]. Comparison of the Fc, Fab, and MAb thermograms in Fig. 2 shows that the large peak for the MAb at both pH values is due to a combination of the Fab peak and the C_H3 peak, while the C_H2 peak from the Fc corresponds to the lower-T peak of the MAb thermogram at pH 4, and the shoulder of the MAb thermogram at pH 6. The overlapping of the DSC curve of the MAb with that of the sum of the Fab and Fc fragments (at equivalent molar conc. to that of the MAb) indicates that the denaturation temperatures of the Fab and Fc domains are not significantly affected by their proximity in the MAb molecule (see Fig. S2 in Supporting information).

Based on the results from DSC for the Fc fragment, temperatures were selected for isothermal aggregation time-course measurements. The temperatures were selected so as to lie above the C_H2 unfolding transition at a given pH, while also lying as far as possible below the C_H3 unfolding peak temperature (T_m). This allowed comparison of MAb aggregation kinetics with those of the fragments at a condition where the fraction of unfolded C_H2 domains is essentially 1, while the C_H3 domains remain folded. No choice of temperature satisfied these criteria while also lying well below the T_m value for Fab unfolding. The insets in panels (a) and (b) of Fig. 2 show monomer loss as a function of incubation time at 60 °C, pH 4.0 and 75 °C, pH 6.0. The monomer loss profile for the Fc fragment at 60 °C and pH 4.0 superimposes quantitatively with that for the MAb. The half-life values (t_{50}) and observed aggregation rate coefficients are indistinguishable within statistical uncertainty. However the monomer loss for the Fab fragment (t_{50} = 625 min) is much slower (~10-fold larger half-life) than that for the MAb (t_{50} = 49.5 min) or Fc (t_{50} = 50.8 min). These results indicate that aggregation is mediated by C_H2 unfolding at this condition. In contrast, at 75 °C and pH 6.0 the aggregation kinetics for intact MAb (t_{50} = 2.88 min) show a slightly smaller half-life than that for Fab fragment (t_{50} = 6.74 min), and a much shorter half-life that than of the Fc fragment (t_{50} = 44.4 min).

Together, these observations indicate that the aggregation of intact MAb is mediated by unfolding of the C_H2 domain at the pH 4 conditions, but not at the pH 6 condition. Furthermore, at pH 6 the incubation temperature is high enough that all the C_H2 domains in the MAb molecules and Fc fragments are unfolded, but is somewhat below the T_m values for unfolding of the Fab or C_H3 domains. This means that a fraction of the MAb molecules have unfolded Fab and/or C_H3 domains at this condition, a fraction of the Fc fragments have unfolded C_H3 domains, and a fraction of the Fab fragments are unfolded. The fraction of molecules with unfolded C_H3 domains is the same for Fc fragments and for MAb molecules, and aggregation of the Fc is much slower than that of MAb. Therefore, C_H3 unfolding does not mediate aggregation for this MAb at either pH 4 or pH 6.

This indicates that Fab unfolding mediates aggregation at the pH 6 conditions. It is proposed that the reason the monomer loss profiles do not overlay quantitatively for Fab aggregation and MAb aggregation at this condition is that the MAb has two branched Fab "arms", compared to a single Fab "arm" per Fab fragment. As a result, there is a statistically higher chance of MAb molecules finding ways to aggregate with each other when compared to just Fab fragments (a simple model to rationalize this is provided in Supporting information). Obtaining pure $(Fab)_2$ fragments was beyond the practical scope of this study, but could be considered to test this hypothesis in future work.

Previous work showed that aggregation is mediated by C_H2 unfolding for some antibodies [30–32], while it is mediated by Fab unfolding for others [25,33]. To the best of our knowledge this is the first report to show that both Fc and Fab are aggregation-prone in the same antibody and, furthermore, that the dominant domain mediating aggregation changes with solution pH for the same protein. Previous computational work hypothesized that there could be more than one aggregation "hot spot" in the same molecule, but that hypothesis was not tested experimentally and all "hot spots" were predicted to be equally aggregation prone [21,19].

In the analysis above and below, it should be noted that the "unfolded" states for Fc and Fab may have significant residual secondary or tertiary structure, as DSC does not provide information on whether a given endotherm corresponds to complete loss of structure for a given domain/region of the protein. Spectroscopic measurements could in principle aid in this regard, however the fact that aggregation occurs on the time scales of the measurements makes it impractical to deduce the precise structural nature of the (partially) unfolded state for aggregation of Fc or Fab fragments, or the intact MAb. By analogy to what has been found for other aggregation-prone proteins, the "unfolded" state or domain may or may not retain significant residual structure [37–43]. In the analysis below focused on the different domains, it is unnecessary to determine the precise structural details of the unfolded (or partially unfolded) state, although this is an interesting question and the focus of future work.

Monomer loss profiles were fit to give the observed rate coefficient (k_{obs}) for monomer loss over the first half-life for each sample condition in the insets of Fig. 2. Observed rate coefficients determined in this way are necessarily a combination of contributions from the intrinsic rate coefficient, k_{int} – i.e., the value of k_{obs} if all monomers were unfolded to reveal their aggregation "hot spots" – and the reduction in the net rate of aggregation due to the fact that only a fraction of monomers are unfolded under most solvent conditions. Mathematically, k_{int} is related to k_{obs} by the following relationship [7,8], $k_{obs} = (f_R)^n\, k_{int}$, where f_R is the fraction of monomers with an unfolded or partially unfolded "reactive" domain at a given solvent condition and temperature, and n is a stoichiometric coefficient that depends on whether aggregation is dominated by dimerization (n = 2) or other mechanisms [44]. For the purposes

of the analysis here, the precise value of n does not affect the results, because in what follows f_R either equals 1 (Fc-mediated aggregation) or is close enough to one for order-of-magnitude analysis (Fab-mediated aggregation).

Table 1 lists the fitted k_{obs} values with their 95% confidence intervals from the non-linear regression. The values of the net charge for the MAb from capillary electrophoresis and sedimentation velocity analytical ultracentrifugation are also given at each pH (see Section Capillary Zone Electrophoresis in Supplemental Material), along with the estimated charge values for Fab and Fc based on the relative amounts of ionizable residues (D, E, H, K, R) in each domain. The value of f_R for aggregation of the C_H2 domain fragments is essentially 1 for both pH 4 and 6 conditions, based on the choice of incubation temperatures relative to C_H2 T_m values at each pH. Therefore, $k_{obs} = k_{int}$ is a good approximation for these conditions, independent of any assumed value for n. To the best of our knowledge, this is first time the intrinsic aggregation rate coefficients associated with C_H2 mediated aggregation have been reported.

These k_{int} values are many orders of magnitude lower than the corresponding diffusion-limited dimerization rate coefficient at this protein concentration (see Supporting information). Interestingly, the value of k_{int} for Fc aggregation is essentially unchanged in moving from pH 4 to pH 6, suggesting that the reduction of net charge (Z^*) by changing pH (cf., Table 1) does not affect the intrinsic aggregation propensity of the unfolded C_H2 domain significantly. This is perhaps not surprising if aggregation is driven by burial of hydrophobic regions of the unfolded C_H2 domain that do not lie close to charged amino acids, or simply if the ionic strength of the solutions here were too high to see significant changes in aggregation rates due to changes in Z^*.

Determining values for k_{int} at pH 4 and 6 for the Fab domain is more difficult, as the unfolding transition for the Fab domain is not fully reversible in DSC at either condition (data not shown). To a first approximation, one can estimate f_R for the Fab domain by taking the fraction of the area of the DSC peak from a baseline temperature up to the incubation temperature for monomer loss kinetics, and then divide that by the total peak area (see Fig. S1 in Supporting information). Doing so gives $f_R = 0.0005$ and 0.12 at pH 4 and 6, respectively. The correct value of n is unknown for Fab aggregation, but typical values lie between 1.5 and 2 [7,44]. Using this range of magnitudes for f_R for Fab aggregation gives k_{int} values that are orders of magnitude larger than those for Fc at either pH.

It should be noted that estimating f_R from the fractional peak area in DSC is at best a semi-quantitative measure, because aggregation consumes unfolded monomer irreversibly and does not allow folding-unfolding equilibrium to be fully achieved during DSC. As a result, the values of f_R determined in this way are likely to be overestimates of the true f_R values [45,46], and so the values for k_{int} in Table 1 are only order of magnitude estimates to illustrate that they are much larger for (partially) unfolded Fab fragments of this IgG1 than for Fc fragments with unfolded C_H2 domains.

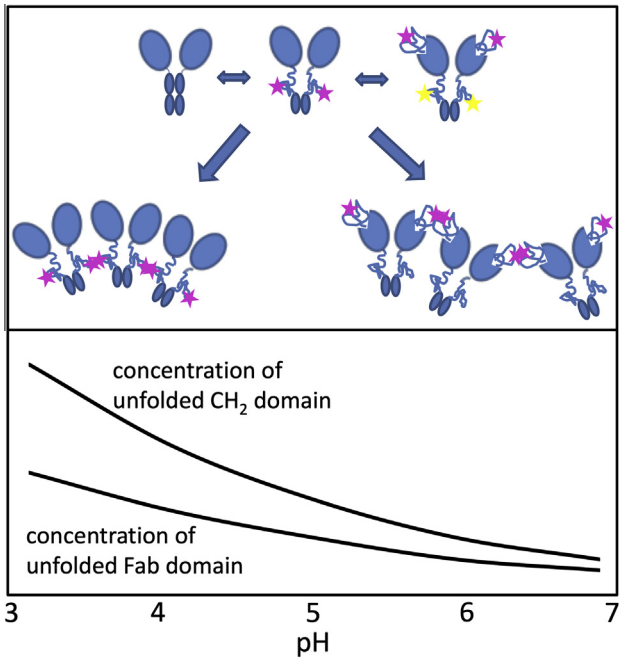

Fig. 3. Schematic depiction of the pH-dependent competition between aggregation pathways. The top panel illustrates that multiple aggregation-prone "hot spots" exist and can be exposed by unfolding of different domains. The bottom panel qualitatively illustrates that the relative concentration of unfolded C_H2 and Fab domains changes to different extents as a function of pH. For the present MAb, the unfolded Fab is more aggregation prone than the unfolded C_H2. Under conditions below the T_m of one or both domains, lowering pH causes a much greater decrease (increase) in the unfolding free energy (unfolded population) for the C_H2 relative to the Fab. This causes a switch from Fab-mediated to C_H2-mediated aggregation at sufficiently acidic pH.

Together, these observations are consistent with the following semi-quantitative mechanistic description (see Fig. 3). Aggregation of this IgG1 occurs through a competition of at least two pathways: one that involves C_H2 unfolding, and the other that involves Fab unfolding. The intrinsic aggregation rates are much higher for the unfolded Fab domain than for the unfolded C_H2 domain, but the thermodynamics of unfolding are sensitive to pH and are different for the different domains (cf., Fig 2). As a result, as one changes solution conditions it is possible to shift from aggregation mediated by unfolding of one domain to that mediated by the other domain. Empirically, the unfolding free energy for the C_H2 domain is typically reduced to a much greater extent by moving to acidic pH than is that for Fab domains [47–49]. As such, it is not surprising in light of the present analysis that Fc-mediated aggregation would become important only at sufficiently low pH for unfolding of the C_H2 domain to occur much more readily than that for Fab domains. The result is a pH-dependent competition between two pathways, with the dominant pathway depending on both the

Table 1
Observed and intrinsic aggregation kinetic rates and net charge of the MAb, Fab and Fc fragments at pH 4 and 6, reported with standard deviation.

Samples	pH 4			pH 6		
	k_{obs} (1/M/Sec)	k_{int} (1/M/Sec)	Z^*	k_{obs} (1/M/Sec)	k_{int} (1/M/Sec)	Z^*
Intact MAb	34 ± 1	467 ± 19	3.2 ± 0.1	187 ± 51	$6 \times 10^3 \pm 2 \times 10^3$	−0.54 ± 0.14
Fab fragment	2.6 ± 0.3	>10[3b]	1.75 ± 0.07[a]	100 ± 4	$7.0 \times 10^3 \pm 0.3 \times 10^3$	−0.30 ± 0.08[a]
Fc fragment	27.1 ± 0.8	27.1 ± 0.8	1.41 ± 0.06[a]	32 ± 8	32 ± 8	−0.24 ± 0.06[a]

[a] Calculated by taking the experimental Z^* value for MAb and scaling it by the ratio of the theoretical net valence for the fragment to that for the intact MAb. See main text for details.

[b] Magnitude of f_R is ~0.001 and n is 1.5–2. It is not reasonable to provide a more accurate estimate of f_R when the value is so low because of limits of signal to noise in the DSC.

intrinsic aggregation rate of a given (partially) unfolded species, and the effective concentration of that species.

The results above show that if one were able to directly compare the aggregation rates of unfolded Fab vs. Fc with unfolded C_H2 domains in a given experimental condition, the unfolded Fab species is more aggregation prone for this IgG1. The choice of temperature and solvent condition helps to control the concentration of those species, and therefore mediates net aggregation rates. As one moves to much lower temperatures than those tested here, it is conceivable that: (i) the identity of the rate-determining step may change, although the identity of the aggregation-prone conformational state or intermediate remains the same (e.g., it may still involve a conformationally disrupted C_H2 domain or Fab); (ii) the dominant pathway for aggregation may change, and then the identity of the key aggregation-prone intermediate may also change.

A change in the rate-determining step (RDS) would alter the net rates of aggregation, but the identity of the "reactive" monomer state would not be expected to change since the RDS would still lie somewhere in the same overall mechanism [50–52]. However, if an alternative pathway for aggregation becomes the lower free-energy-barrier pathway at lower temperature (e.g., via adsorption to air–water or solid–liquid interfaces) [53], then it is possible that the identity of the key aggregation-prone, partially unfolded monomer state for a given antibody would switch from high vs. low temperature. Although beyond the scope of the present report, future work will focus on aggregation mechanisms over a wide temperature range and in the presence of other stresses that could alter mechanisms/key intermediates.

In terms of the implications of the above results for other monoclonal antibodies, one must consider that the Fc is essentially conserved across all members of the same subclass (e.g., IgG1 in this case), but the Fab is not. As a result, one could encounter antibodies with Fab domains that have much higher or lower k_{int} values than the antibody tested here. While engineering variable regions in the Fab domain to decrease k_{int} of intact IgG1 molecules could be a strategy to improve resistance of these molecules to aggregation, the results here highlight that there is a limit to how effective this can be. That is, if one lowers k_{int} for Fab domains sufficiently far, eventually k_{int} combined with f_R for the Fab domain will fall below that of the C_H2 domain for a given monoclonal antibody. This argues that improving the intrinsic aggregation propensity of the unfolded C_H2 (and possibly C_H3) domains should also be considered when one seeks to improve aggregation resistance by protein engineering, as has been done for non-IgG antibodies [23] and for other proteins [26].

Acknowledgements

The authors thank Boehringer Ingelheim Pharmaceuticals Inc. for financial support and the supply of protein. The funding source was not involved in: study design; collection, analysis and interpretation of data; writing of the report; and in the decision to submit the article for publication.

Appendix A. Supplementary data

Supplementary data associated with this article can be found, in the online version, at http://dx.doi.org/10.1016/j.febslet.2014.01.051.

References

[1] Carter, P. (2011) Introduction to current and future protein therapeutics: a protein engineering perspective. Exp. Cell Res. 317, 1261–1269.
[2] Braun, A., Kwee, L., Labow, M. and Alsenz, J. (1997) Protein aggregates seem to play a key role among the parameters influencing the antigenicity of interferon alpha (IFN-alpha) in normal and transgenic mice. Pharm. Res. 14, 1472–1478.
[3] Schellekens, H. (2002) Bioequivalence and the immunogenicity of biopharmaceuticals. Nat. Rev. 1, 457–462.
[4] Goswami, S., Wang, W., Arakawa, T. and Ohtake, S. (2013) Developments and challenges for mAb-based therapeutics. Antibodies 2, 452–500.
[5] Liu, H., Ma, J., Winter, C. and Bayer, R. (2010) Recovery and purification process development for monoclonal antibody production. mAbs 2, 480–499.
[6] Latypov, R., Hogan, S., Lau, H., Gadgil, H. and Liu, D. (2012) Elucidation of acid-induced unfolding and aggregation of human immunoglobulin IgG1 and IgG2 Fc. J. Biol. Chem. 287, 1381–1396.
[7] Roberts, C. (2007) Non-native protein aggregation kinetics. Biotechnol. Bioeng. 98, 9237–9238.
[8] Roberts, C. (2003) Kinetics of irreversible protein aggregation: analysis of extended Lumry-Eyring models and implications for predicting protein shelf life. J. Phys. Chem. B 107, 1194–1207.
[9] Fink, A. (1998) Protein aggregation: folding aggregates, inclusion bodies and amyloid. Fold. Des. 3, R9–R23.
[10] Uversky, V. and Fink, A. (2004) Conformational constraints for amyloid fibrillation: the importance of being unfolded. Biochim. Biophys. Acta 1698, 131–153.
[11] Eisenberg, D. et al. (2006) The structural biology of protein aggregation diseases: fundamental questions and some answers. Acc. Chem. Res. 39, 568–575.
[12] Groot, N., Pallares, I., Avilés, F., Vendrell, J. and Ventura, S. (2005) Prediction of 'hot spots' of aggregation in disease-linked polypeptides. BMC Struct. Biol. 5, 18, http://dx.doi.org/10.1186/1472-6807-5-18.
[13] Pawar, A. et al. (2005) Prediction of 'aggregation-prone' and 'aggregation-susceptible' regions in proteins associated with neurodegenerative diseases. J. Mol. Biol. 350, 379–392.
[14] Morimoto, A. et al. (2004) Analysis of the secondary structure of beta-amyloid (Abeta42) fibrils by systematic proline replacement. J. Biol. Chem. 279, 52781–52788.
[15] Scrocchi, L. et al. (2003) Identification of minimal peptide sequences in the (8–20) domain of human islet amyloid polypeptide involved in fibrillogenesis. J. Struct. Biol. 141, 218–227.
[16] Zhang, A. et al. (2010) Molecular level insights into thermally induced alpha-chymotrypsinogen A amyloid aggregation mechanism and semiflexible protofibril morphology. Biochemistry (Mosc.) 49, 10553–10564.
[17] Giasson, B., Murray, I., Trojanowski, J. and Lee, V. (2001) A hydrophobic stretch of 12 amino acid residues in the middle of alpha-synuclein is essential for filament assembly. J. Biol. Chem. 276, 2380–2386.
[18] Ivanova, M., Sievers, S., Sawaya, M., Wall, J. and Eisenberg, D. (2009) Molecular basis for insulin fibril assembly. PNAS 106, 18990–18995.
[19] Wang, X., Das, T., Singh, S. and Kumar, S. (2009) Potential aggregation prone regions in biotherapeutics. mAbs 1, 254–267.
[20] Conchillo-Solé, O. et al. (2007) AGGRESCAN: a server for the prediction and evaluation of 'hot spots' of aggregation in polypeptides. BMC Bioinformatics 8.
[21] Fernandez-Escamilla, A., Rousseau, F., Schymkowitz, J. and Serrano, L. (2004) Prediction of sequence-dependent and mutational effect on the aggregation of peptides and proteins. Nat. Biotechnol. 22, 1302–1306.
[22] Rouet, R., Lowe, D. and Christ, D. (2014) Stability engineering of the human antibody repertoire. FEBS Lett. 588 (2), 269–277.
[23] Wörn, A. and Plückthun, A. (2001) Stability engineering of antibody single-chain Fv fragments. J. Mol. Biol. 305, 989–1010.
[24] He, F., Hogan, S., Latypov, R., Narhi, L. and Razinkov, V. (2009) High throughput thermostability screening of monoclonal antibody formulations. J. Pharm. Sci. 99, 1707–1720.
[25] Sahin, E., Grillo, A., Perkins, M. and Roberts, C. (2010) Comparative effects of pH and ionic strength on protein–protein interactions, unfolding, and aggregation for IgG1 antibodies. J. Pharm. Sci. 99, 4830–4848.
[26] Sahin, E. et al. (2011) Computational design and biophysical characterization of aggregation-resistant point mutation for γD cyrstallin illustrate a balance of conformational stability and intrinsic aggregation propensity. Biochemistry (Mosc.) 50, 628–639.
[27] Bork, P., Holm, L. and Sander, C. (1994) The immunoglobulin fold, structural classification, sequence patterns and common core. J. Mol. Biol. 242, 309–320.
[28] Demarest, S., Rogers, J. and Hansen, G. (2004) Optimization of the antibody CH3 domain by residue frequency analysis of IgG sequences. J. Mol. Biol. 335, 41–48.
[29] Gauci, P. and Alderton, M. (2001) Pepsin digestion of antibodies to produce functional antigen-binding fragments (Fab): a scientific fantasy. Def. Sci. Technol. Organ., 1–47. **(TR-1189)**.
[30] Andersen, C., Manno, M., Rischel, C., Thorolfsson, M. and Martorana, V. (2010) Aggregation of a multidomain protein: a coagulation mechanism governs aggregation of a model IgG1 antibody under weak thermal stress. Protein Sci. 19, 279–290.
[31] Gong, R. et al. (2009) Engineered human antibody constant domains with increased stability. J. Biol. Chem. 284, 14203–14210.
[32] Liu, H., Chumasae, C., Gaza-Bulseco, G. and Goedken, E. (2010) Domain-level stability of an antibody monitored by reduction, differential alkylation, and mass spectrometry analysis. Anal. Biochem. 400, 244–250.
[33] Brummitt, R. et al. (2011) Nonnative aggregation of an IgG1 antibody in acidic conditions: part 1. unfolding, colloidal interactions, formation of high-molecular-weight aggregates. J. Pharm. Sci. 100, 2087–2103.

[34] Malmborg, A., Ellmark, P., Borrebaeck, C. and Furebring, C. (2003) Affinity and epitope profiling of mouse anti-CD40 monoclonal antibodies. Scand. J. Immunol. 57, 517–524.
[35] Souillac, P. (2005) Biophysical characterization of insoluble aggregates of a multi-domain protein: an insight into the role of the various domains. J. Pharm. Sci. 94, 2069–2083.
[36] Ionescu, R., Vlasak, J., Price, C. and Kirchmeier, M. (2008) Contribution of variable domains to the stability of humanized IgG1 monoclonal antibodies. J. Pharm. Sci. 97, 1414–1426.
[37] Grillo, A. et al. (2001) Conformational origin of the aggregation of recombinant human factor VIII. Biochemistry (Mosc.) 40, 586–595.
[38] Krishnan, S. et al. (2002) Aggregation of granulocyte colony stimulating factor under physiological conditions: characterization and thermodynamic inhibition. Biochemistry (Mosc.) 41, 6422–6431.
[39] Hamarstrom, P. et al. (1999) Structural mapping of an aggregation nucleation site in a molten globule intermediate. J. Biol. Chem. 274, 32897–32903.
[40] Lindner, R., Treweek, T. and Carver, J. (2001) The molecular cheaperone alpha-crystallin is in kinetic competition with aggregation to stabilize a monomeric molten-globule form of alpha-lactalbumin. Biochem. J. 354, 79–87.
[41] Finke, J., Roy, M., Zimm, B. and Jennings, P. (2000) Aggregation events occur prior to stable intermediate formation during refolding of interleukin 1beta. Biochemistry (Mosc.) 39, 575–583.
[42] Khurana, R. et al. (2001) Partially folded intermediates as critical precursors of light chain amyloid fibrils and amorphous aggregates. Biochemistry (Mosc.) 40, 3525–3535.
[43] Rucker, A. and Creamer, T. (2002) Polyproline II helical structure in protein unfolded states: lysine peptides revisited. Protein Sci. 11, 980–985.
[44] Andrews, J. and Roberts, C. (2007) A Lumry-Eyring nucleation plymerization model of protein aggregation kinetics: 1. aggregation with pre-equilibrated unfolding. J. Phys. Chem. B 111, 7897–7913.
[45] Sanchez-Ruiz, J., Lopez-Lacomba, J., Cortijo, M. and Mateo, P. (1988) Differential scanning calorimetry of the irreversible thermal denaturation of thermolysin. Biochemistry (Mosc.) 27, 1648–1652.
[46] Sanchez-Ruiz, J. (1992) Theoretical analysis of Lumry-Eyring models in differential scanning calorimetry. Biophys. J. 61, 921–935.
[47] Buren, N., Rehder, D., Gadgil, H., Matsumura, M. and Jacob, J. (2009) Elucidation of two major aggregation pathways in an IgG2 antibody. J. Pharm. Sci. 98, 3013–3030.
[48] Vermeer, A. and Norde, W. (2000) The thermal stability of immunoglobulin: unfolding and aggregation of a multi-domain protein. Biophys. J. 78, 394–404.
[49] Tischenko, V., Abramov, V. and Zav'yaloov, V. (1998) Investigation of the cooperative structure of Fc fragments from myeloma immunoglobulin G. Biochemistry (Mosc.) 37, 5576–5581.
[50] Roberts, C. and Darrington, R. (2003) Irreversible aggregation of recombinant bovine granulocyte-colony stimulating factor (bG-CSF) and implications for predicting protein shelf life. J. Pharm. Sci. 92, 1095–1111.
[51] Andrews, J. and Roberts, C. (2007) Non-native aggregation of alpha-Chymotrypsinogen occurs through nucleation and growth with competing nucleus sizes and negative activation energies. Biochemistry (Mosc.) 46, 7558–7571.
[52] Weiss IV, W., Young, T. and Roberts, C. (2009) Principles, approaches, and challenges for predicting protein aggregation rates and shelf life. J. Pharm. Sci. 98, 1246–1277.
[53] Bee, J. et al. (2012) Production of particles of therapeutic proteins at the air–water interface during compression/dilation cycles. Soft Matter 8, 10329–10335.